

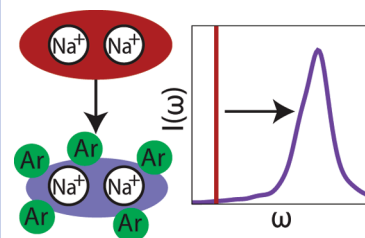
# How Does a Solvent Affect Chemical Bonds? Mixed Quantum/Classical Simulations with a Full CI Treatment of the Bonding Electrons

William J. Glover,<sup>§</sup> Ross E. Larsen,<sup>†</sup> and Benjamin J. Schwartz\*

Department of Chemistry and Biochemistry, University of California, Los Angeles, Los Angeles, California 90095-1569

**ABSTRACT** Understanding how a solvent affects the quantum mechanics and reactivity of the chemical bonds of dissolved solutes is of fundamental importance to chemistry. To explore condensed-phase effects on a simple molecular solute, we have studied the six-dimensional two-electron wave function of the bonding electrons of the Na<sub>2</sub> molecule in liquid argon via mixed quantum/classical simulation. We find that even though Ar is an apolar liquid, solvent interactions produce dipole moments on Na<sub>2</sub> that can reach magnitudes over 1.4 D. These interactions also change the selection rules, induce significant motional-narrowing, and cause a large (26 cm<sup>-1</sup>) blue shift of the dimer's vibrational spectrum relative to that in the gas phase. These effects cannot be captured via classical simulation, highlighting the importance of quantum many-body effects.

**SECTION** Statistical Mechanics, Thermodynamics, Medium Effects



Understanding how a solvent affects the quantum mechanics and reactivity of the chemical bonds of dissolved solutes is of fundamental importance to chemistry. The solvent's influence on chemical bonds arises from alteration of a solute's electronic structure due to both short- and longer-ranged interactions with hundreds of nearby solvent molecules. This solvent-induced alteration of the solute's electronic structure can alter the vibrational frequencies and/or dissociation energies of the solute's chemical bonds. Traditional molecular dynamics (MD) simulations based on classical pairwise additive force fields are unable to explore the detailed physics underlying the solvent's influence on chemical bonds because such simulations cannot account for changes in the solute's electronic structure with the environment. Classical models can be improved by adding many-body polarization terms; it has recently been shown that such terms are necessary to successfully reproduce the vibrational spectrum of liquid water and ice.<sup>1,2</sup> It is unclear, however, whether classical polarizable models can universally describe the changes in the solute electronic structure that alter the nature of bond vibrations. This is particularly true in nonpolar systems where longer-ranged electrostatic interactions play a much smaller role than inherently quantum mechanical interactions such as Pauli repulsion. To capture these effects, the quantum mechanics of the solute valence electrons responsible for the chemical bonding and the interactions of these electrons with the surrounding solvent molecules must be accounted for at the Hamiltonian level. There has been some semiempirical work done to include solvent effects on the bonding electronic structure in simulations examining the photodissociation dynamics of I<sub>2</sub> in rare gas liquids/matrixes<sup>3,4</sup> and I<sub>2</sub><sup>-</sup> in rare gas and CO<sub>2</sub> clusters,<sup>5-7</sup> but to the best of our knowledge,

there has been no first-principles treatment of solvent–solute chemical bond interactions for diatomics in simple liquids.

In this paper, we go beyond a semiempirical treatment of the solute's electronic structure and use first-principles quantum mechanics to calculate the influence of a solvent on the electrons in a chemical bond. We avoid the formidable task of solving Schrödinger's equation (SE) for all of the electrons on both the solvent and solute molecules in the simulation by adopting a mixed quantum/classical (MQC) approach, in which we solve the SE exactly for the valence electrons of a diatomic solute. Due to the relative simplicity of its electronic structure, we have chosen the sodium dimer (Na<sub>2</sub>) as our solute, and we have investigated the chemical bond dynamics of Na<sub>2</sub> dissolved in liquid argon. This leads to a computational problem that involves finding the electronic states of the two Na<sub>2</sub> valence electrons in the presence of hundreds of classical Ar atoms and two Na<sup>+</sup> core particles. We solve this problem using our recently developed two-electron Fourier grid (2EFG) method, which is outlined for this particular application in the Supporting Information (SI). We find that even though liquid Ar is an apolar solvent, its influence on the bonding electrons of Na<sub>2</sub> is quite substantial; nonpolar interactions with Ar atoms that push the valence electrons off of the nuclear centers produce a large instantaneous dipole moment on the dimer that can reach magnitudes of over 0.3 e–Å (1.4 D). The presence of the solvent-induced fluctuating dipole leads to both a new far-IR absorption feature and an alteration of the selection rules for the dimer's infrared vibrational absorption.

**Received Date:** October 5, 2009

**Accepted Date:** November 2, 2009

Moreover, the solvent-induced alteration of the bonding electron density between the Na<sub>2</sub> nuclei leads to a large (26 cm<sup>-1</sup>) blue shift of the dimer's bond vibration relative to that in the gas phase. Classical simulations are unable to account for this shift of the bond vibrational frequency because purely classical force fields do not capture the solvent-induced alteration of the Na<sub>2</sub> bonding electron density.

Our MQC approach to simulating Na<sub>2</sub> in liquid Ar involves finding the ground-state solution to the SE for the two sodium dimer valence electrons in the potential of all of the classical solvent atoms. The SE was solved using our recently developed 2EFG method (see SI). Briefly, the valence electrons' wave function was represented on a six-dimensional real space grid, and the SE was solved variationally at every molecular dynamics time step. The simulation cell was cubic with a side of 43.8332 Å and contained 1600 classical Ar atoms, 2 classical Na<sup>+</sup> cations, and 2 fully quantum mechanical electrons. Our model for the Na<sub>2</sub> intramolecular interactions is described in the SI and involves a Phillips–Kleinman electron–Na<sup>+</sup> pseudopotential<sup>8</sup> and classical Coulombic repulsion between the two Na<sup>+</sup> nuclei. The solute–solvent coupling was taken from Gervais et al.<sup>9</sup> with a slight modification of their solvent polarization potential (see SI). We modeled the classical Ar–Ar interactions with Lennard-Jones (LJ) potentials.<sup>10</sup> The simulation time step was 5 fs ( $\sim 2.3 \times 10^{-5}$  reduced LJ time units), and the classical particles were propagated with the velocity Verlet algorithm<sup>10</sup> in the microcanonical ensemble; for our simulation cell, the Ar reduced density was 0.75, and after equilibration, the Ar temperature was  $120 \pm 4$  K (reduced temperature close to 1.0), placing the Ar solvent in the liquid region of the LJ phase diagram.<sup>11</sup> The electrons' wave function was expressed on a 16<sup>6</sup> cubic grid (i.e., a configuration interaction (CI) basis of  $\sim 1.7 \times 10^7$  functions) that spanned 14 Å in each direction and was centered in the middle of the simulation cell where the Na<sub>2</sub> was located. Data were collected from a production run of 500 ps. All of the simulation parameters and the details of the calculations involved are described in the SI.

To provide a point of reference, we began by investigating the electronic structure of the gas-phase sodium dimer with the same level of theory as that used for our condensed-phase simulations. The solid black curve in Figure 1 shows the Born–Oppenheimer potential energy curve (PEC) for the sodium dimer's bond displacement computed using our 2EFG method, where the zero of energy was chosen to be twice the energy of Na<sup>0</sup> calculated with the same grid basis. Despite our choice of a grid basis for a problem with cylindrical symmetry, the calculated PES is smooth, exhibits a clear minimum at  $R_e = 3.27$  Å with depth  $D_e = 0.679$  eV, and goes to zero at large displacement, indicating that the 2EFG method correctly calculates electronic structure at all distances including the dissociation limit, as expected for a CI-based method. The second derivative of the PEC at the minimum corresponds to a harmonic oscillator frequency of  $\omega_e = 136$  cm<sup>-1</sup>. These values compare well with previous theory at a similar level to our model but using Gaussian basis functions, which found  $R_e = 3.34$  Å,  $D_e = 0.458$  eV, and  $\omega_e = 136$  cm<sup>-1</sup>.<sup>12</sup>

Having seen that the 2EFG method provides a reasonably good description of the electronic structure of gas-phase Na<sub>2</sub>,

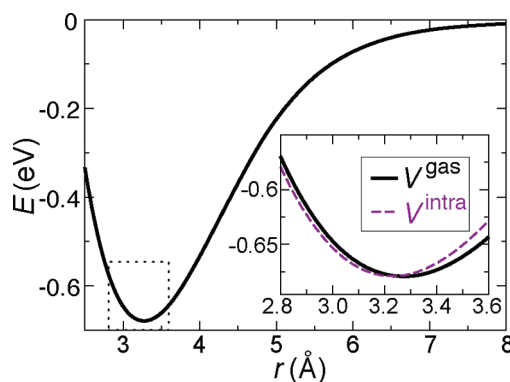


**Figure 1.** Gas-phase potential energy curve for the sodium dimer. The inset expands the region around the minimum and also plots the solvent-averaged intramolecular potential,  $\langle V^{\text{intra}}(r) \rangle$  (purple dashed curve), described in the text.

we now use this method to consider the properties of the dimer dissolved in liquid Ar. Perhaps the largest surprise from these calculations is that immersion of Na<sub>2</sub> into simulated liquid Ar leads to the presence of a substantial instantaneous electric dipole moment,  $\mu(t)$ , on the dimer, the properties of which are plotted in Figure 2. Figure 2A plots a time trace of  $|\mu(t)|$  from a portion of our simulation. This figure makes it clear that there are large fluctuations in  $|\mu(t)|$ , reaching values of over 0.3 e–Å (1.4 D), with an ensemble average value of  $\sim 0.1$  e–Å ( $\sim 0.5$  D). The presence of such large dipole moments is quite surprising since liquid Ar is apolar and thus expected to be a weakly interacting solvent; this is the main reason that it and other noble gases are used in matrix isolation studies. Since there are no charges on the solvent to polarize the electrons on the dimer, the observed dipole moment must result from short-ranged interactions with the solvent. These “overlap-induced dipoles” result from the Pauli repulsion between the Ar and Na<sub>2</sub> electrons,<sup>13</sup> an effect included in our simulations via the e<sup>-</sup>–Ar pseudopotential. Interestingly, even though classical studies have shown that nonpolar solvation is dominated by only a few close solvent atoms,<sup>14</sup> the magnitude and direction of the induced dipole depends on the positions of multiple Ar atoms relative to the sodium dimer, as we show explicitly in the SI. This means that quantum mechanical many-body effects are important in determining the induced dipole.

To better understand the consequences of the dipole on Na<sub>2</sub> induced by the solvent, we investigated the time dependence of the instantaneous dipole moment by calculating the dipole time autocorrelation function,  $C(t) = \langle \mu(t) \cdot \mu(0) \rangle$ , which is shown in Figure 2B. The fact that interactions with the solvent produce a fluctuating dipole moment with substantial memory gives rise to an interaction-induced absorption spectrum, which we calculated in the classical limit (via eq 2.10 of ref 13) and plotted in Figure 2C. The spectrum shows a peak in the far-IR at  $\sim 50$  cm<sup>-1</sup>, which is well separated from the dimer's solution-phase oscillator frequency and presumably results from intramolecular rattling motions of the dimer in the solvent cage, similar to interpretations of the far-IR spectrum of H<sub>2</sub> in liquid Ar.<sup>15</sup> The weaker feature at  $\sim 160$  cm<sup>-1</sup>, which is expanded in the inset of

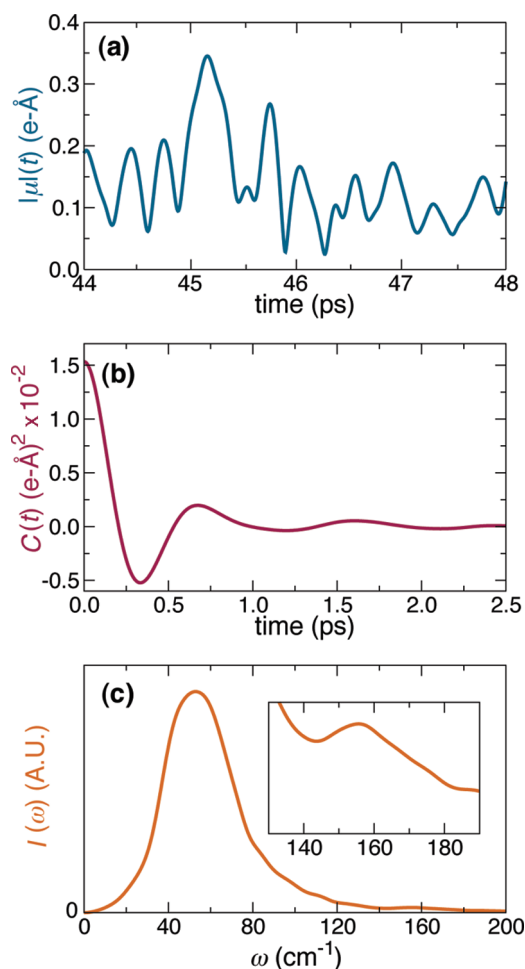


**Figure 2.** Properties of the instantaneous induced dipole moment on  $\text{Na}_2$  in liquid Ar. (a) Time trace of the induced dipole moment,  $\mu(t)$ , from a portion of our MQC simulation. (b) Dipole autocorrelation function averaged over the 500 ps simulation. (c) Absorption spectrum of  $\text{Na}_2$  induced from the fluctuating dipole. The inset highlights the contribution from  $\text{Na}_2$ 's intramolecular vibrational frequency at around  $160 \text{ cm}^{-1}$ .

Figure 2C, occurs at the bond frequency of the dimer; many-body interactions with the solvent cause the normally symmetry-forbidden infrared vibrational absorption of the dimer to become weakly allowed in the presence of the Ar solvent.

In addition to creating a fluctuating dipole moment at the bond vibrational frequency, the change in electronic structure of the dimer induced by the solvent also alters the fundamental nature of the bond vibration. The blue solid curve in Figure 3 shows the power spectrum,  $\tilde{C}(\omega)$ , of the bond velocity autocorrelation function for MQC-simulated  $\text{Na}_2$  in liquid Ar. The green dashed curve shows the same spectrum calculated from a 1 ns all-classical simulation of this system in which the  $\text{Na}_2$  bond was described by a quartic fit to the gas-phase  $\text{Na}_2$  PEC shown in Figure 1 and the solute–solvent interactions were represented by a three-center fit to our calculated  $\text{Na}_2$ –Ar gas-phase potential energy surface (see SI). For reference, the natural harmonic frequency of the gas-phase dimer in our model is shown as the black vertical dotted line. The all-classical and MQC power spectra have peaks that are

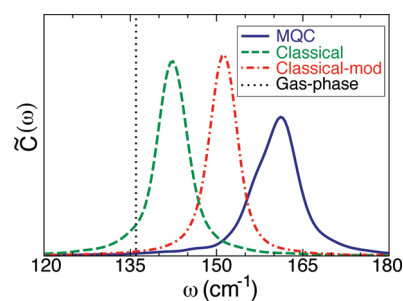


**Figure 3.** Vibrational spectrum of  $\text{Na}_2$  calculated from the Fourier transform of the bond velocity autocorrelation function. Solid blue curve: from the mixed quantum/classical simulation. Dashed green curve: from the classical simulation, with a three-site potential. Dot-dashed red curve: from the classical simulation with a modified intramolecular potential as described in the text. Dotted black line: gas-phase vibrational frequency.

blue shifted from the gas phase by 7 and  $26 \text{ cm}^{-1}$ , respectively; the solvent clearly has a substantial effect on the  $\text{Na}_2$  bond vibration. The small blue shift seen in the all-classical simulation results from physical confinement of the vibrating solute; the presence of the solvent near the outer turning point of the vibration effectively steepens the potential holding the diatomic together, resulting in a small increase in the vibrational frequency. However, the fact that the all-classical simulation underestimates the magnitude of the vibrational blue shift seen in the MQC simulation by a factor of  $\sim 4$  indicates that many-body quantum effects that alter the electronic structure of the dimer are far more important in determining the bond vibrational frequency.

The origin of these many-body effects on the bond vibrational frequency can be seen by simply considering the spatial extent of the bonding electrons' wave function; when the dimer bond length is  $3.2 \text{ \AA}$ , the mean radius of gyration of the quantum valence electrons' charge density for gas-phase  $\text{Na}_2$  is  $2.61 \text{ \AA}$ , while that for  $\text{Na}_2$  in liquid Ar is only  $2.42 \text{ \AA}$ . This is consistent with a picture in which the solvent particles compress the electron density between the Na nuclei, leading to a stiffer chemical bond. This solvent compression of the bonding electrons also decreases the average  $\text{Na}_2$  bond length from  $3.27 \pm 0.01 \text{ \AA}$  in the all-classical simulation to  $3.17 \pm 0.01 \text{ \AA}$  in the MQC simulation. Thus, the vibrational blue shift of  $\text{Na}_2$  dissolved in liquid Ar results primarily from many-body electronic effects that cannot be adequately modeled with a classical, gas-phase parametrization, even when all of the classical interactions are derived from quantum mechanical calculations.

To further explore the origin of the vibrational blue shift of  $\text{Na}_2$  in liquid Ar, we separated the Born–Oppenheimer potential energy of the dimer into two parts,  $V^{\text{NaNa}} = V^{\text{inter}} + V^{\text{intra}}$ . The first term contains operators that depend only on solvent degrees of freedom,  $V^{\text{inter}} = \langle \psi | \hat{V}^{\text{Ar}} | \psi \rangle + U^{\text{Na}^+-\text{Ar}}$ , in which  $\hat{V}^{\text{Ar}}$  is the argon–electron potential operator and  $U^{\text{Na}^+-\text{Ar}}$  is the total sodium–argon classical potential. The second term contains operators that depend on the solute's degrees of freedom,  $V^{\text{intra}} = \langle \psi | \hat{V}^{\text{Na}} + \hat{T} | \psi \rangle + 1/R$ , in which  $\hat{V}^{\text{Na}}$  is the sodium–electron potential operator,  $\hat{T}$  is the kinetic energy operator for the electrons, and  $R$  is the dimer bond length. Even though the presence of  $\psi$  in the expectation value causes  $V^{\text{intra}}$  to implicitly

depend on the coordinates of the solvent (i.e., there is still some many-body character in this potential that has not been completely removed), we chose this particular separation since in the limit of no solvent interactions,  $V^{\text{intra}}$  reduces precisely to the gas-phase Born–Oppenheimer  $\text{Na}_2$  potential (i.e., the solid curve in Figure 1). In the presence of solvent, this separation allows us to generate an effective condensed-phase intramolecular potential for the dimer by calculating  $V^{\text{intra}}(r)$  for many solvent configurations by holding the solvent fixed while mapping out  $V^{\text{intra}}$  along the bond displacement and then ensemble averaging over the different solvent configurations. This solvent-averaged intramolecular potential energy surface,  $\langle V^{\text{intra}}(r) \rangle$ , is plotted as the purple dashed curve in the inset to Figure 1; for reference, the gas-phase PEC of the dimer is shown as the solid black curve. A comparison of the two curves shows that solvent interactions both shift the intramolecular potential minimum to a shorter bond length and increase the curvature at the minimum. Thus, interactions with the solvent that compress the electronic wave function are responsible for both the decreased bond length and increased vibrational frequency of  $\text{Na}_2$  in solution.

We note that if we construct another all-classical simulation of this system in which we use  $\langle V^{\text{intra}}(r) \rangle$  instead of the gas-phase PEC as the intramolecular dimer potential, the vibrational spectrum of the dimer blue shifts an additional  $\sim 9 \text{ cm}^{-1}$ , as shown by the red dot–dashed curve in Figure 3. This modified classical simulation, which incorporates some of the quantum effects of the solvent on the solute, clearly provides a better portrayal of the vibrational properties of the dimer in the condensed phase than that when the gas-phase potential is used, but the modified classical simulation is still unable to account for all of the shift seen in the full MQC simulation. Thus, many-body effects in the intermolecular part of the potential, which cannot be easily incorporated into classical simulations, are important in a correct description of the dynamics of chemical bonds in condensed phases.

Figure 3 shows that not only does interaction with the solvent change the average vibrational frequency of the dimer, but it also changes the width of the vibrational resonance; the full width at half-maximum of the peak in the vibrational power spectrum increases from  $4.6 \text{ cm}^{-1}$  in the all-classical simulations (green dashed and red dot–dashed curves) to  $5.8 \text{ cm}^{-1}$  in the MQC simulation (solid blue curve). The contributions from the physical processes underlying the width of a vibrational peak in a condensed-phase system can be fairly difficult to tease apart.<sup>16</sup> Probably the simplest contribution to the spectral width is inhomogeneous broadening; different solvent configurations around the solute will result in a static vibrational spectrum that is broadened from the gas phase due to a distribution of instantaneous vibrational frequencies. Of course, if the solvent motions that shift the vibrational frequency are sufficiently rapid, the spectral line width will decrease due to motional narrowing. For both our MQC and classical systems, we calculated the inhomogeneous contributions to the vibrational power spectrum by calculating the distribution of frequencies associated with the instantaneous second derivative of the PEC. We found that in both the MQC and classical systems, the intrinsic inhomogeneous line width of  $\text{Na}_2$  in liquid Ar was  $28 \text{ cm}^{-1}$ . This is substantially broader than the actual vibrational spectrum

including solvent dynamics, indicating that the vibrational spectrum of  $\text{Na}_2$  in liquid Ar is significantly motional narrowed. The fact that the classical simulation predicts even narrower vibrational resonances is a sign that there is either too much motional narrowing in the classical simulation or that the contribution from vibrational energy relaxation (which is included classically in all three of our simulations) is different between the MQC and all-classical simulations.

In conclusion, we have applied our two-electron Fourier grid electronic structure method to simulate the chemical bond dynamics of the sodium dimer in liquid argon. By allowing the solvent to directly interact with the bonding electrons in the solute, we have been able to investigate a whole host of many-body effects that alter the properties of the molecule relative to the gas phase. The most substantial change upon solvation of  $\text{Na}_2$  in liquid Ar is the development of a large instantaneous dipole moment that both creates a new far-IR absorption at frequencies characteristic of the solute rattling motions and changes the selection rules to allow (gas-phase forbidden) absorption at the solute's vibrational frequency. Compression of the bonding electrons by the surrounding solvent particles also increases the electron density between the solute nuclei, leading to a vibrational frequency that is more blue shifted than an all-classical simulation would predict. We also saw that even with potentials derived from quantum calculations and a  $\text{Na}_2$  intramolecular potential adjusted for a condensed-phase environment, classical simulations were still unable to reproduce the vibrational dynamics of  $\text{Na}_2$ , highlighting the sensitivity of chemical bonds to many-body interactions that only a first-principles-based quantum calculation can capture. Finally, we note that although we have focused entirely on the properties of the solute in its ground electronic state in this paper, our 2EFG method also produces accurate electronic excited states, opening the exciting possibility of performing first-principles quantum simulations of the photodissociation dynamics of chemical bonds in condensed-phase environments.

**SUPPORTING INFORMATION AVAILABLE** Full details of all the simulation models presented in this publication and exploration of the origin of  $\text{Na}_2$ 's induced dipole moment in more detail. This material is available free of charge via the Internet at <http://pubs.acs.org>.

## AUTHOR INFORMATION

### Corresponding Author:

\*To whom correspondence should be addressed. E-mail: [schwartz@chem.ucla.edu](mailto:schwartz@chem.ucla.edu).

### Present Addresses:

<sup>§</sup> Department of Chemistry, Stanford University.

<sup>†</sup> National Renewal Energy Laboratory, Golden CO.

**ACKNOWLEDGMENT** This work was supported by the National Science Foundation under Grants CHE-0603766 and CHE-0908548 and the American Chemical Society Petroleum Research Fund under Grant 45988-AC,6. We gratefully acknowledge the California



NanoSystems Institute and the UCLA Institute for Digital Research and Education for use of their Beowulf clusters.

## REFERENCES

- (1) Burnham, C. J.; Anick, D. J.; Mankoo, P. K.; Reiter, G. F. The Vibrational Proton Potential in Bulk Liquid Water and Ice. *J. Chem. Phys.* **2008**, *128*, 154519.
- (2) Mankoo, P. K.; Keyes, T. POLIR: Polarizable, Flexible, Transferable Water Potential Optimized for IR Spectroscopy. *J. Chem. Phys.* **2008**, *129*, 034503.
- (3) Batista, V. S.; Coker, D. F. Nonadiabatic Molecular Dynamics Simulation of Photodissociation and Geminate Recombination of I<sub>2</sub> Liquid Xenon. *J. Chem. Phys.* **1996**, *105*, 4033–4054.
- (4) Batista, V. S.; Coker, D. F. Nonadiabatic Molecular Dynamics Simulation of Ultrafast Pump–Probe Experiments on I<sub>2</sub> in Solid Rare Gases. *J. Chem. Phys.* **1997**, *106*, 6923–6941.
- (5) Faeder, J.; Delaney, N.; Maslen, P. E.; Parson, R. Charge Flow and Solvent Dynamics in the Photodissociation of Cluster Ions: A Nonadiabatic Molecular Dynamics Study of I<sub>2</sub><sup>-</sup>·Ar<sub>n</sub>. *Chem. Phys. Lett.* **1997**, *270*, 196–205.
- (6) Delaney, N.; Faeder, J.; Maslen, P. E.; Parson, R. Photodissociation, Recombination, and Electron Transfer in Cluster Ions: A Nonadiabatic Molecular Dynamics Study of I<sub>2</sub><sup>-</sup>(CO<sub>2</sub>)<sub>n</sub>. *J. Phys. Chem. A* **1997**, *101*, 8147.
- (7) Maslen, P. E.; Faeder, J.; Parson, R. An Effective Hamiltonian for an Electronically Excited Solute in a Polarizable Molecular Solvent. *Mol. Phys.* **1998**, *94*, 693–706.
- (8) Glover, W. J.; Larsen, R. E.; Schwartz, B. J. The Roles of Electronic Exchange and Correlation in Charge-Transfer-to-Solvent Dynamics: Many-Electron Non-Adiabatic Mixed Quantum/Classical Simulations of Photoexcited Sodium Anions in the Condensed Phase. *J. Chem. Phys.* **2008**, *129*, 164505.
- (9) Gervais, B.; Giglio, E.; Jacquet, E.; Ipatov, A.; Reinhard, P.-G. Simple DFT Model of Clusters Embedded in Rare Gas Matrix: Trapping Sites and Spectroscopic Properties of Na Embedded in Ar. *J. Chem. Phys.* **2004**, *121*, 8466–8480.
- (10) Allen, M. P.; Tildesley, D. J. *Computer Simulation of Liquids*; Oxford University Press: London, U.K., 1992.
- (11) Smit, B. Phase Diagrams of Lennard-Jones Fluids. *J. Chem. Phys.* **1992**, *96*, 8639.
- (12) Liu, Z.; Carter, L. E.; Carter, E. A. Full Configuration Interaction Molecular Dynamics of Na<sub>2</sub> and Na<sub>3</sub>. *J. Phys. Chem.* **1995**, *99*, 4355–4359.
- (13) Birnbaum, G.; Guillot, B.; Bratos, S. Theory of Collision-Induced Line-Shapes—Absorption and Light-Scattering at Low-Density. *Adv. Chem. Phys.* **1982**, *51*, 49–112.
- (14) Larsen, R. E.; David, E. F.; Goodyear, G.; Stratt, R. M. Instantaneous Perspectives on Solute Relaxation in Fluids: The Common Origins of Nonpolar Solvation Dynamics and Vibrational Population Relaxation. *J. Chem. Phys.* **1997**, *107*, 524–543.
- (15) Buontempo, U.; Cunsolo, S.; Dore, P. Far Infrared Spectra of H<sub>2</sub> in Liquid Ar and Memory Effects in the Translational Bands. *J. Chem. Phys.* **1975**, *62*, 4062.
- (16) Kalbfleisch, T.; Keyes, T. Untangling the Physical Contributions to Instantaneous Normal Mode Approximations: Inhomogeneous Broadening, Motional Narrowing, And Energy Relaxation. *J. Chem. Phys.* **1998**, *108*, 7375–7383.